

Understanding the Implications of a LINAC's Microstructure on Transient Photocurrent Models

M. L. McLain¹, J. K. McDonald¹, T. J. Sheridan¹, E. F. Hartman¹, V. Harper-Slaboszewicz¹,
and C. Hembree¹

¹Sandia National Laboratories, Albuquerque, NM

ABSTRACT:

The implications of a linear accelerator's microstructure (i.e., train of narrow pulses) on transient photocurrent models are investigated. Typically, the rate the energy is deposited in a material during the microstructure peaks is much higher than the pulse-averaged rate.

Corresponding (and Presenting) Author:

Michael L. McLain
Sandia National Laboratories
P.O. Box 5800, MS 1167, Albuquerque, NM, 87185-1167
Phone: 505-844-6825
Email: mlmcrai@sandia.gov

Co-Authors:

Kyle McDonald	Sandia National Labs*	Email: jkmcdon@sandia.gov	Phone: 505-845-7939
Tim Sheridan	Sandia National Labs*	Email: tjsheri@sandia.gov	Phone: 505-845-7942
Fred Hartman	Sandia National Labs*	Email: efhart@sandia.gov	Phone: 505-845-3473
Chuck Hembree	Sandia National Labs*		
Vic Harper-Slaboszewicz		Email: vjharpe@sandia.gov	Phone: 505-844-1062

Session Preference: Basic Mechanisms, Hardness Assurance, or Dosimetry,

Presentation Preference: Oral

Classification: Unlimited Release

FUNDING STATEMENT

Sandia National Laboratories is a multi-program laboratory managed and operated by Sandia Corporation, a wholly owned subsidiary of Lockheed Martin Corporation, for the U.S. Department of Energy's National Nuclear Security Administration under contract DE-AC04-94AL85000.

INTRODUCTION

Linear accelerators (LINAC) are a common source used to study transient radiation effects in devices and circuits as well as to gather data for model development. The reason for this is that LINACs are typically capable of producing repeatable and predictable radiation output over long periods of time (i.e., reproducible pulsing over a week of experiments), and a significant amount of pulsed exposures can occur over a week of experiments compared to other pulsed-power sources. However, the output of a LINAC typically consists of a train of narrow pulses (i.e., microstructure) that can complicate the interpretation of the radiation diagnostics and devices under test [1]. More specifically, the rate the energy is deposited (i.e., dose rate) in a material during the microstructure peaks is much higher than the pulse-averaged dose rate which is traditionally captured (refer to Fig. 1). If a material or device is able to respond to high-frequency, short-duration pulses, this may result in inherent inaccuracies in transient photocurrent models developed with LINAC data. Moreover, upset and/or burnout could potentially occur at lower thresholds than expected. Therefore, it is critical to understand the impact of the microstructure on any device tested at a LINAC, and as necessary, capture those effects during model development and the verification and validation (V&V) process. In this summary, the implications of the microstructure on transient photocurrent models for p-n junctions are investigated. These models are a key component in radiation aware photocurrent models that would be implemented in a circuit simulator.

EXPERIMENTAL AND MODELING DETAILS

Experimental data was obtained at the Medusa LINAC located at the Little Mountain Test Facility (LMTF). The Medusa LINAC is an L-band radio frequency (RF) electron accelerator that contains a Klystron system that provides power to the accelerating waveguides and operates at a frequency of 1.28 GHz. Similar to the basic electron LINAC design, the electrons are generated from a thermionic DC gun biased at 50 kV. Following the gun are pre-bunchers, a focusing lens, the L-band accelerating column, and the exit port. Experimenters have the option to place a scatter plate and/or a Bremsstrahlung target that can be used to generate X-rays, at the end of the exit port. Here, a 0.125 in. scatter plate was placed at the end of the exit port and the LINAC was operated in electron-beam mode. The Medusa LINAC provides a nominal electron energy of 20 MeV for varying pulse widths ($50 \text{ ns} \leq \text{PW} \leq 100 \mu\text{s}$) and dose rates. In these experiments, the pulse width was set to either 50 ns or 1 μs . For a more in depth description of the basic principles of linear accelerators refer to [2].

Diamond and Gallium Arsenide (GaAs) photoconductive detectors (PCDs) were used to characterize the temporal profile of the radiation pulse. In a PCD, the electric potential applied across the absorbing region causes a current to flow that is proportional to the irradiance. An example of a filtered signal captured

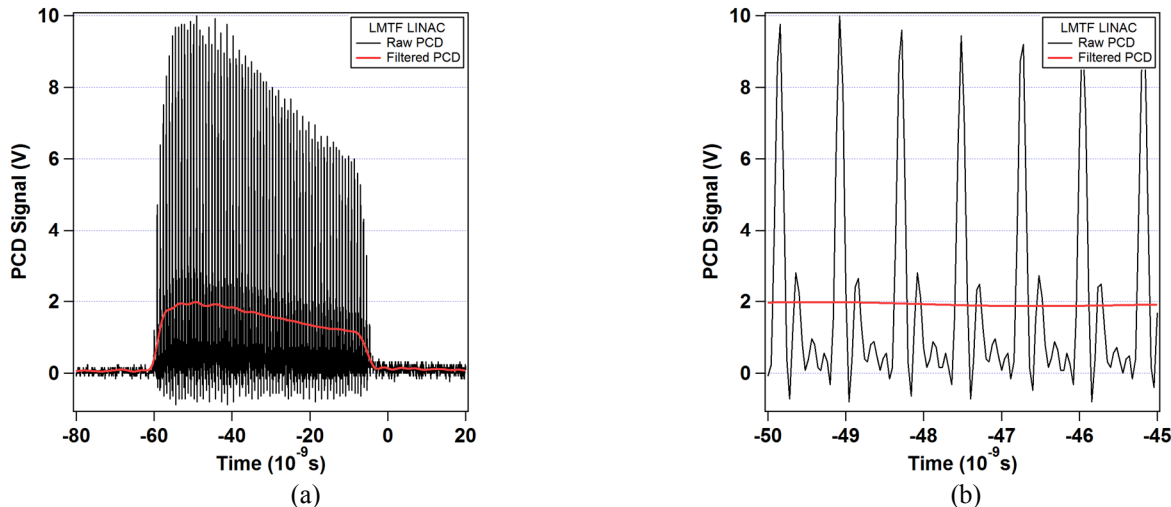


Fig. 1. Plots of the raw and filtered Diamond PCD signals for a 50 ns pulse on (a) a full time scale and (b) zoomed-in view. The unfiltered PCD signal has a 1.28 GHz pulse frequency with $\sim 125 \text{ ps}$ wide pulses.

by a GaAs and diamond PCD at the Medusa LINAC is shown in Fig. 1 and Fig. 2(a), respectively. Note that the PCD signal can be filtered during post-processing or measurement. During measurement, a combination of long cable lengths and filtering on the oscilloscope results in the averaging of the 1.28 GHz microstructure. Also shown in Fig. 1 are plots of the raw GaAs PCD signal revealing the microstructure. Indeed, there is a significant difference between the raw and filtered GaAs PCD signal. More specifically, the unfiltered PCD signal has a 1.28 GHz pulse frequency and each pulse has an approximate full width at half maximum (FWHM) of 125 ps. The duty factor is $\sim 15\%$ and the rise and fall times of each pulse is on the order of 100 ps. Also notice that the raw PCD microstructure peaks are up to 80% greater in magnitude than the time-averaged, filtered signal. During this radiation exposure, the pulse width was 50 ns.

Typically, transient photocurrent models are created using the pulse-averaged temporal profile. The question is, however, does not capturing the microstructure impact the accuracy of the photocurrent model? Several papers have discussed different methods of modeling the photocurrent response of a p-n junction over the past few decades [3-6]. In this summary, we will implement the Fjeldy model within Matlab and investigate the impact of the microstructure on the photocurrent response. The basic equation governing the total photocurrent density can be expressed as [3]

$$J_{photo} = J_{prompt} + J_{n,delay} + J_{p,delay} \quad (1)$$

where J_{prompt} is the prompt photocurrent density, $J_{n,delay}$ is the diffusion-based n-type delayed photocurrent contribution, and $J_{p,delay}$ is the diffusion-based p-type delayed photocurrent contribution. The delayed photocurrent components are related to the buildup and discharge of charge carriers in the two quasi-neutral regions adjacent to the junction [3]. In (1),

$$J_{prompt} = qGW_{dep}, \quad (2)$$

$$J_{n,delay} = G_n L_{nd}, \quad (3)$$

and

$$J_{p,delay} = G_p L_{pd} \quad (4)$$

where q is the absolute value of the electron charge, G , G_n , and G_p are the carrier generation rates, W_{dep} is the width of the depletion region, and L_{nd} and L_{pd} are the effective diffusion lengths for electrons and holes, respectively. The photocurrent can be determined by simply multiplying the photocurrent density by the area. For more details about the model refer to [3].

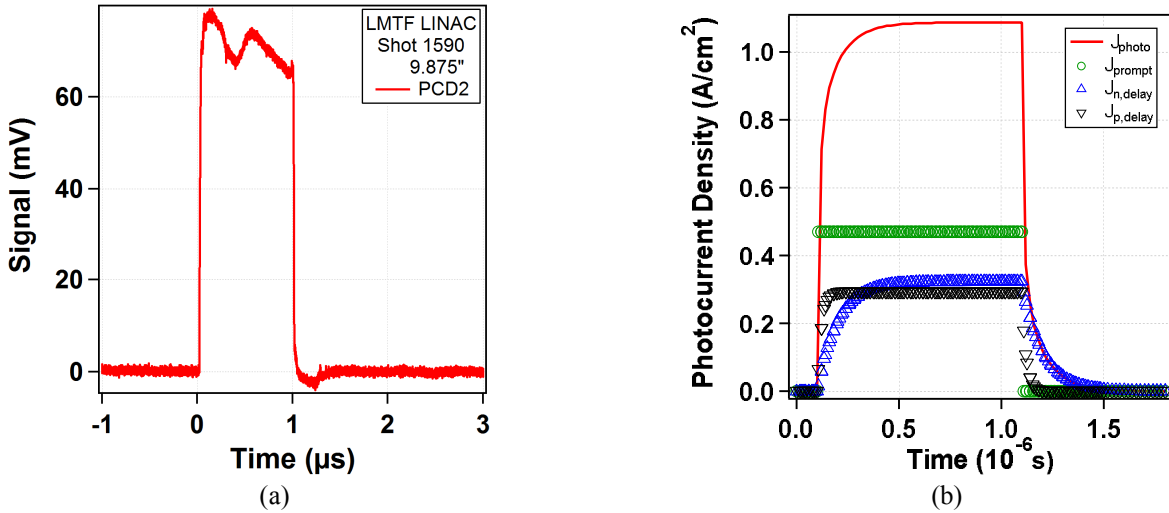


Fig. 2. (a) Plot of a filtered diamond PCD signal at a distance of ~ 25 cm (9.875 in) from the exit port. The 1.28 GHz microstructure does not appear in the PCD signal due to long cable lengths and filtering on the scopes. (b) Photocurrent response calculated using the Fjeldy method assuming a square wave pulse similar to what is shown in (a).

RESULTS AND DISCUSSION

Using (1), the photocurrent density was calculated for a p-n junction assuming the radiation exposure was a $1 \mu\text{s}$ square wave pulse. This pulse shape would be similar to the time-averaged, diamond PCD signal shown in Fig. 2(a). The calculated total, prompt, and delayed photocurrent density components are presented in Fig. 2(b). Observe that the prompt and delayed components are comparable. Depending on the values selected for the parameters within the model, this may not always be the case. Shown in Fig. 3(a) is the calculated raw and filtered normalized photocurrent for a 50 ns pulse (based on the PCD data in Fig. 1). As expected, the photocurrent response follows the PCD shape since the generation rate terms in (2) through (4) are directly proportional to the dose rate and thus the PCD temporal profile. The slight shift in the filtered signal is due to the filtering process of the raw signal. If the raw signal is smoothed using a boxcar smooth algorithm (refer to Fig. 3(b)), the predicted photocurrent response is similar to the filtered photocurrent response. This suggests that if a material, device, or circuit is not capable of responding to the microstructure, there is not a reason to capture its effect in a photocurrent model.

Shown in Fig. 4 are experimental data obtained on an Si-based NPN bipolar junction transistor (BJT) used in RF applications. As observed in the plot, the RF BJT was capable of responding to the high-frequency, short duration pulses produced by the LINAC. This resulted in larger photocurrents during each microstructure peak compared to the filtered photocurrent ($\sim 5\times$ at the peak). The reason for this is that the effective carrier generation rate (i.e., dose rate) is higher at the microstructure peaks. This is potentially problematic if an upset/burnout threshold is surpassed or if one is trying to establish the aforementioned thresholds for radiation hardness assurance reasons. Furthermore, if these effects are not properly captured in the model development and V&V process, the photocurrent models provided to circuit designers may not be accurate. As discussed previously, not all devices will respond to the high-frequency component associated with the LINAC microstructure. However, it is reasonable to assume that many RF devices and circuits could be impacted by the microstructure. In addition to that, materials such as GaAs are known to be able to respond to the microstructure. In the final paper and presentation, other technologies will be considered. Additionally, numerical simulations will be conducted using Silvaco's device simulator and compared to the analytical model and observed experimental response.

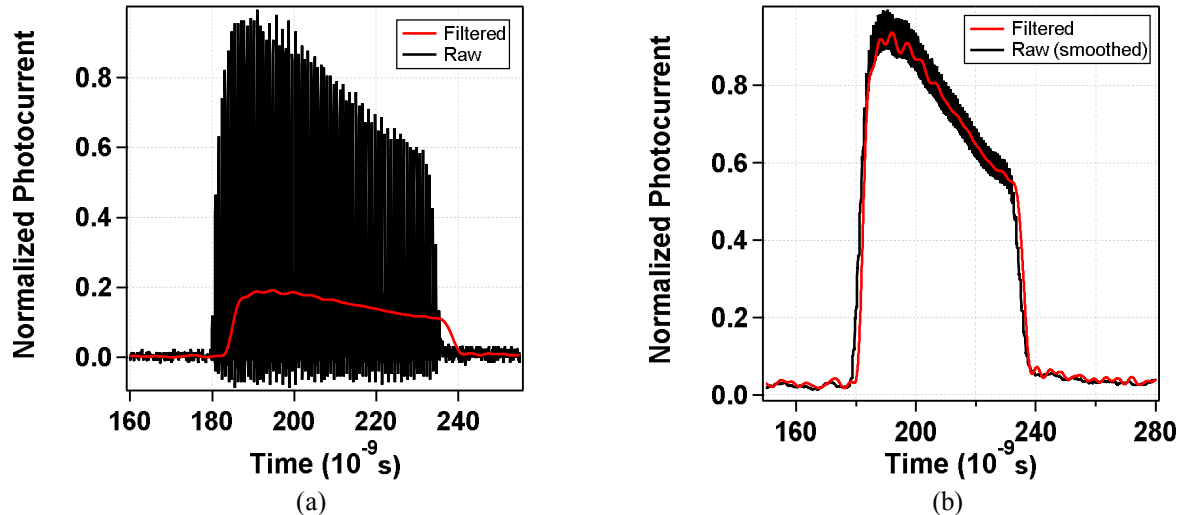


Fig. 3. (a) Plot of the calculated raw and filtered normalized photocurrents for a 50 ns pulse (based on the PCD data in Fig. 1). (b) Plot comparing the calculated raw photocurrent boxcar smoothed to the filtered photocurrent.

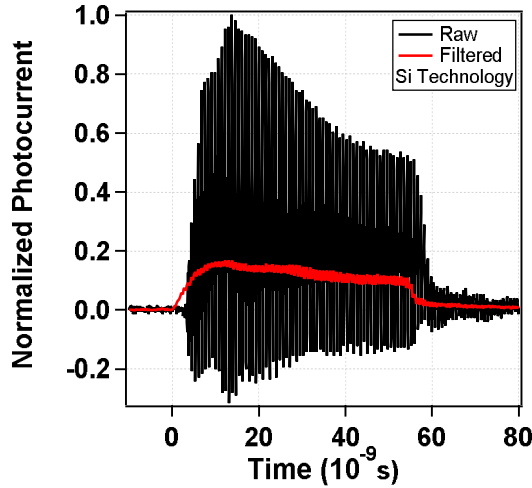


Fig. 4. Plot of the raw and filtered normalized photocurrent for a RF Si transistor. The observed response follows the temporal profile of the PCD.

CONCLUSION

When creating radiation aware photocurrent models for transistors and circuits, it is imperative to understand the radiation diagnostics characterizing the radiation source as well as the response of the device or circuit. With respect to the microstructure characteristic of electron LINACs, it is necessary to account for this in models and transient radiation studies when the technology (e.g., GaAs or Si RF devices) is capable of responding to high-frequency, short duration pulses. As shown in this summary for an RF Si BJT, the photocurrent response was $\sim 5\times$ greater when accounting for the microstructure. Thus, modeling the microstructure is a key component for that technology. This not only has implications for model development, but also for accurately determining upset/burnout thresholds.

REFERENCES

- [1] V. J. Harper-Slaboszewicz, "Dosimetry experiments at the Medusa Facility (Little Mountain)," Sandia National Laboratories, Albuquerque, NM, SAND Report SAND2010-6771 2010.
- [2] T. P. Wangler, *RF Linear Accelerators*: Wiley, 2008.
- [3] T. A. Fjeldly, Y. Deng, M. S. Shur, H. P. Hjalmarson, A. Muyshondt, and T. Ytterdal, "Modeling of high-dose-rate transient ionizing radiation effects in bipolar devices," *IEEE Trans. on Nucl. Sci.*, vol. 48, no. 5, pp. 1721-1730, 2001.
- [4] J. L. Wirth and S. C. Rogers, "The transient response of transistors and diodes to ionizing radiation," *IEEE Trans. on Nucl. Sci.*, vol. 11, no. 5, pp. 24-38, 1964.
- [5] E. W. Enlow and D. R. Alexander, "Photocurrent modeling of modern microcircuit pn junctions," *IEEE Trans. on Nucl. Sci.*, vol. 35, no. 6, pp. 1467-1474, 1988.
- [6] C. L. Axness, B. Kerr, and T. F. Wunsch, "Analytic light—or radiation—induced pn junction photocurrent solutions to the multidimensional ambipolar diffusion equation," *Journal of Applied Physics*, vol. 96, no. 5, pp. 2646-2655, 2004.